Intuitive physical reasoning about objects' masses transfers to a visuomotor decision task consistent with Newtonian physics

Nils Neupärtl[1,2], Fabian Tatai[1,2], Constantin A. Rothkopf[1,2,3*]

1 Centre for Cognitive Science, Technical University Darmstadt, 64283 Darmstadt, Germany
2 Institute of Psychology, Technical University Darmstadt, 64283 Darmstadt, Germany
3 Frankfurt Institute for Advanced Studies, Goethe University, 60438 Frankfurt, Germany

* constantin.rothkopf@cogsci.tu-darmstadt.de

Abstract

While interacting with objects during every-day activities, e.g. when sliding a glass on a counter top, people obtain constant feedback whether they are acting in accordance with physical laws. However, classical research on intuitive physics has revealed that people's judgements systematically deviate from predictions of Newtonian physics. Recent research has explained these deviations not as consequence of misconceptions about physics but instead as the consequence of the probabilistic interaction between inevitable perceptual uncertainties and prior beliefs. How intuitive physical reasoning relates to visuomotor actions is much less known. Here, we present an experiment in which participants had to slide pucks under the influence of naturalistic friction in a simulated virtual environment. The puck was controlled by the duration of a button press, which needed to be scaled linearly with the puck's mass and with the square-root of initial distance to reach a target. Over four phases of the experiment, uncertainties were manipulated by altering the availability of sensory feedback and providing different degrees of knowledge about the physical properties of pucks. A hierarchical Bayesian model of the visuomotor sliding task incorporating perceptual uncertainty and press-time variability found substantial evidence that subjects adjusted their button-presses so that the sliding was in accordance with Newtonian physics. After observing collisions between pucks, subjects transferred the relative masses inferred perceptually to adjust subsequent sliding actions. Crucial in the modeling was the inclusion of a cost function, which quantitatively captures participants' implicit sensitivity to errors due to their motor variability. Taken together, in the present experiment we find evidence that our participants transferred their intuitive physical reasoning to a subsequent visuomotor control task in accordance with Newtonian physics and weigh potential outcomes with cost functions based on their knowledge about their own variability.

Author summary

During our daily lives we interact with objects around us governed by Newtonian physics. While people are known to show multiple systematic errors when reasoning about Newtonian physics, recent research has provided evidence that this is the

consequence of perceptual uncertainties and partial knowledge about object properties. Here, we carried out an experiment to investigate whether people transfer their intuitive physical reasoning to how they interact with objects. Using a simulated virtual environment in which participants had to slide different pucks into a target region by the length of a button press, we found evidence that they could do so in accordance with the underlying physical laws. Moreover, our participants watched movies of colliding pucks and subsequently transferred their beliefs about the relative masses of the observed pucks to the sliding task. Remarkably, this transfer was consistent with Newtonian physics and could well be explained by a computational model that takes participants' perceptual uncertainty, action variability, and preferences into account.

Introduction

Whether sliding a glass containing a beverage on a counter top in your kitchen or shooting a stone on a sheet of ice in curling, acting successfully in the world needs to take physical relationships into account. While humans intuitively sense an understanding of the lawful relationships governing our surroundings, research has disputed that this is indeed the case [1, 2]. Instead, human judgements and predictions about the dynamics of objects deviate systematically from the laws of Newtonian mechanics. Past research has interpreted these misjudgments as evidence that human judgements violate the laws of physics and that they instead use context specific rules of thumb, so called heuristics [2–4]. E.g., when judging relative masses of objects such as billiard balls based on observed collisions, people seem to use different features of motion in different contexts and end up with erroneous predictions [2].

But recent research has provided a different explanation of human misjudgments on the basis of the fact that inferences in general involve sensory uncertainties and ambiguities, both in perceptual judgements [5, 6] as well as in reasoning and decision making [7, 8]. Therefore, physical reasoning needs to combine uncertain sensory evidence with prior beliefs about physical relationships to reach predictions or judgements [9–12]. By probabilistically combining prior beliefs and uncertain observations, a posterior probability about the unobserved physical quantities is obtained. Judgements and predictions are then modeled as based on these probabilistic inferences. Thus, deviations from the predictions of Newtonian physics in this framework are attributed to perceptual and model uncertainties.

This framework of explaining reasoning about physical systems on the basis of Newtonian mechanics and perceptual uncertainties has been referred to as the noisy Newton framework (see e.g. [13] for a review). It has been quite successful at explaining a range of discrepancies between predictions of Newtonian physics and human predictions for various perceptual inference tasks. E.g., when observing simulated collisions of objects with different masses, subjects' biases in judgements of mass ratios agree well with physical predictions, if the perceptual uncertainties are included [9, 14]. Additionally, the noisy Newton framework can also explain why human judgements depend on experimental paradigms, because tasks differ in the availability of knowledge about objects' properties [15]. E.g., this suggests an explanation for the fact that judgements about physical situations based on a static image representing a situation at a single timepoint have usually been reported to deviate more from physical ground truth compared to richly animated stimuli [16], which additionally allow to estimate objects' velocities.

While physical reasoning has been studied predominantly using tasks in which subjects needed to judge physical quantities or predict how objects continue to move, much less is known about how intuitive physical reasoning guides actions. Commonly, experimental paradigms have asked subjects to judge physical properties such as

relative masses in two-body collisions [3, 9, 11, 12], predict the future trajectory of an object when no action is taken based on an image of a situation at a single timepoint, such as a pendulum [15], a falling object [17], or whether an arrangement of blocks is stable [12]. Other experiments have asked subjects to predict a trajectory of objects [18] or their landing position [10] after seeing an image sequence, but again without subjects interacting with the objects in the scene. By contrast, the literature on visuomotor decisions and control [19–22] has seldom investigated the relationship between visuomotor decisions, actions, and control and physical reasoning. Notable exceptions are studies, which have investigated how humans use internal models of gravity in the interception of moving targets [23] and how exposure to 0-gravity environments [24] changes this internal model. Other studies have investigated how perceptual judgements and visuomotor control in picking up and holding objects in the size-weight and material-weight illusions can be dissociated [25, 26]. Nevertheless, these studies did not investigate the relationship of intuitive physical reasoning and visuomotor actions.

Here we investigate how human subjects guide their actions based on their beliefs about physical quantities given prior assumptions and perceptual observations. Thus, we combine work on intuitive physics [9, 11, 12] and visuomotor control [19, 21, 23, 25]. First, do humans use the functional relationships between physical quantities as prescribed by Newtonian mechanics in new task situations? E.g., when sliding an object on a surface the velocity with which the object needs to be released needs to scale linearly with the object's mass but with the square-root of the distance the object needs to travel. Second, after having observed collisions between objects do humans adjust their actions in accordance with the inferred relative masses of those objects? E.g., while it is known that subjects can judge mass ratios of two objects when observing their collisions, it is unclear whether they subsequently use this knowledge when sliding those objects. To address these questions, subjects were asked to shoot objects gliding on a surface under the influence of friction to hit a target's bullseye in a simulated virtual environment. The simulated puck was accelerated by subjects' button presses such that the duration of a button press was proportional to the puck's release velocity. A succession of five conditions investigated, what prior assumptions subjects had about the relationships between physical quantities, whether they could learn to adjust to different masses when visual feedback about their actions was available, and whether they could use mass ratios inferred from observing collisions to adjust their actions.

Analysis of the data shows that subjects adjusted their press-times depending on the distance the pucks had to travel. Furthermore, subjects adjusted the button press-times to get closer to the target within a few trials when visual feedback about the puck's motion was available. Because perceptual uncertainties and motor variability can vary substantially across subjects and to take Weber-Fechner scaling into account, we subsequently analyzed the data with a hierarchical Bayesian model under the assumption that subjects used a Newtonian physics based model and compared it to the prediction of a linear heuristics model. Importantly, because subjects needed to adjust their button press-times, the model needs to account for perceptual judgements and the selection of appropriate actions. We include a comparison of three costs functions to investigate subjects' selection of press-times. Based on this model of the sliding task, we find evidence that subjects used the functional relationship between mass and distance of pucks as prescribed by Newtonian physics. Moreover, biases in subjects' press-times can be explained as stemming from costs for not hitting the target, which grow quadratically with the distance of the puck to the target's bullseye. After observing 24 collisions between an unknown puck and two pucks with which subjects had previously interacted, we found evidence that participants transferred the inferred relative masses to subsequent sliding actions. Thus, intuitive physical reasoning transfers from perceptual judgements to control tasks and deviations from the predictions of

Newtonian physics are not only attributable to perceptual and model uncertainties but also to subjects' implicit costs for behavioral errors.

Materials and methods

Participants

Twenty subjects took part in the experiment. All participants were undergraduate or graduate students recruited at the Technical University Darmstadt, who received course credit for participation. All experimental procedures were carried out in accordance with the guidelines of the German Psychological Society and approved by the ethics committee of the Darmstadt University of Technology. Informed consent was obtained from all participants prior to carrying out the experiment. All subjects had normal or corrected to normal vision and were seated so that their eyes were approximately 40 cm away from the display and the monitor subtended 66 degrees of visual angle horizontally and 41 degrees vertically. In the vertical direction the monitor had a resolution of 1080 pixels, which corresponded to a distance of approximately $11.5m$ in the simulation. Four participants have been excluded from the analysis (three due to incorrect task execution and one due to incomplete data; f=9, m=11, age=[18,27], median=22.5, mean=22.25).

Experimental design and data

Participants were instructed to shoot a puck in a virtual environment into the bullseye of a target, similar to an athlete in curling. The shot was controlled by the duration of pressing a button on a keyboard. Participants were told that they were able to adjust the force, which initially was going to accelerate the puck and thus the initial velocity of the puck, by the duration of their press. Additionally, participants were told that realistic friction was going to slow down the puck while sliding on the simulated surface. The general objective of the experimental design was to investigate whether subjects adjusted their shooting of the pucks in a way that was in line with the physical laws governing motion under friction. Specifically, the magnitude of the initial impulse exerted on the puck determines how far the puck slides on the surface. Thus, subjects needed to adjust the duration of a button press according to the distance between the randomly chosen initial position of the puck and the target on each trial. The different experimental phases allowed investigating subjects' prior beliefs about the puck's dynamics, their adjustments of button presses when these beliefs were updated given visual feedback of the puck's motion, and the potential transfer of knowledge about relevant object properties to the control of the puck from perceiving object collisions. Therefore we designed a task with two conditions and four consecutive experimental phases, which differed in the availability of previous knowledge and feedback.
**Laws of motion governing the puck's motion.** At the beginning of each trial, subjects saw the fixed target and a puck resting at a distance chosen uniformly at random between one and five meters from the target's bullseye. To propel the puck toward the target, subjects needed to press a button. To model the relationship between the button press and the puck's motion, we reasoned as follows. Human subjects have been shown to be able to reason accurately about the mass ratio of two objects when observing elastic collisions between them [9]. In elastic collisions, according to Newtonian laws, the impulse transferred by the collision is proportional to the interaction duration with a constant force. In other words, the duration of the interaction with a constant force leads to a linearly scaled impulse. Given a constant mass m of a puck and assuming a constant surface friction coefficient μ, Newtonian physics allows deriving the button press-time T_{press} required to propel the puck to the

target at a distance Δx:

$$T_{press} = \sqrt{\frac{2\mu gm^2}{F^2}\Delta x} \propto m \cdot \sqrt{\Delta x} \qquad (1)$$

with gravitational acceleration g and a constant force F. Here, the constant force F is being applied by the interaction, i.e. the button press of duration T_{press}, which is physically equivalent to an elastic collision with an object. Note that this formulation of the interaction has the additionally intuitive consequence that the release velocity of the puck scales linearly with the duration of the button press (see S1 Appendix "Puck Movement"). The second expression clarifies, that the press-time scales linearly with the mass of the puck, while it scales with the square-root of the distance to the target. Obviously, this relationship assumes perfect knowledge of all involved quantities. The
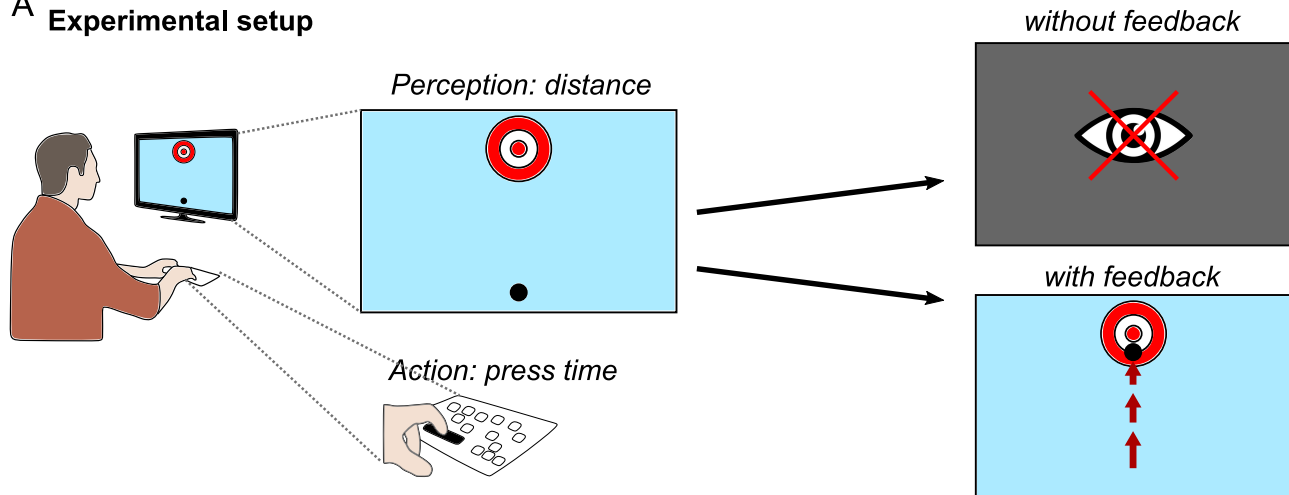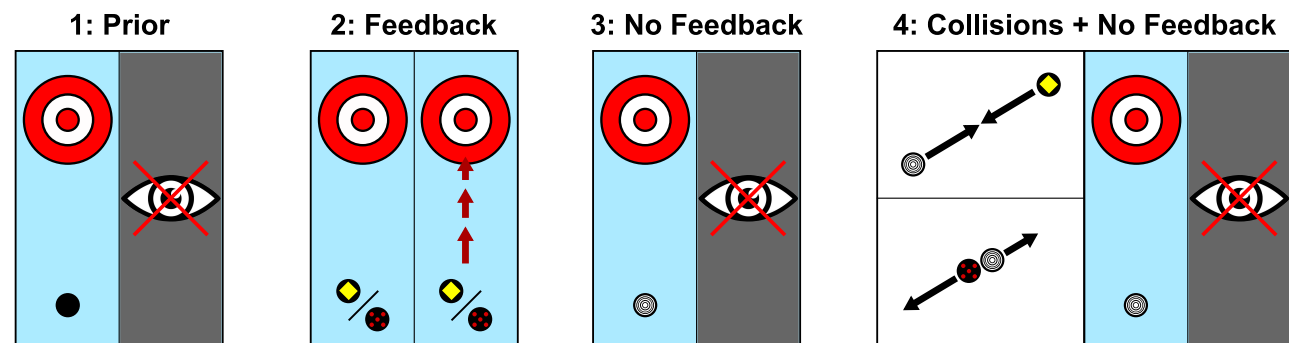

Fig 1. Task design. (A) Single trial illustration. Target area and puck are presented on a monitor from bird's-eye perspective. Releasing the pressed button accelerates the puck by applying a force, which is proportional to the press-time. In trials without feedback the screen turned black after button release, while in feedback trials participants were able to see the puck moving according to simulated physics. **(B)** Four phases of experiment. In the 'prior' phase, no feedback about puck motion was available, whereas in the 'feedback' phase subjects obtained visual feedback about the pucks' motion. Two pucks with different color and correspondingly different masses were simulated. In the 'no feedback' phase subjects obtained a new puck as indicated by an unknown color and obtained no feedback. In the last phase, subjects first watched 24 collisions between the new puck and the pucks they had interacted with in the 'feedback' phase before interacting again with the puck. Note that the puck of the 'no feedback' and 'collisions + no feedback' phase are identical.

movement of the puck was implemented by simulating the equivalent difference $_{164}$
equations for each frame given the friction and the velocity of the preceding frame $_{165}$
(detailed derivations are provided in the S1 Appendix, "Puck Movement"). $_{166}$

Phase 1: Prior beliefs. In the first phase, we wanted to investigate, which functional $_{167}$
relationship subjects would use a priori to select the duration of button presses $_{168}$
depending on the perceived distance between the puck and the target. A black puck $_{169}$
with unknown mass m was placed at a distance to the target drawn uniformly at $_{170}$
random. Participants received no further information about the puck or the $_{171}$
environment. Participants were instructed to press the button in a way so as to bring $_{172}$
the puck into the target area, but after pressing the button for a duration t^{pre} and $_{173}$
releasing it the screen turned black to mask the resulting movement of the puck. This $_{174}$
screen lasted for at least half a second until the participant started the next trial by $_{175}$
button press. All participants carried out fifty trials. Thus, the collected data allowed $_{176}$
relating different initial puck distances to the press-times subjects selected based on $_{177}$
their prior beliefs. $_{178}$

Phase 2: Visual feedback. The second phase was designed to investigate, how $_{179}$
participants adjusted their button press-times in relation to the simulated masses of $_{180}$
pucks and their initial distances to the target when visual feedback about the pucks' $_{181}$
motion was available. To this end, participants carried out the same puck-shooting task $_{182}$
but with two different pucks, as indicated by distinct surface textures (yellow diamond $_{183}$
versus five red dots, see fig 1 b, *Feedback*). The two pucks were alternating every four $_{184}$
trials with a total number of two-hundred trials. The two different pucks were simulated $_{185}$
with having differing masses, resulting in different gliding dynamics. In this condition, $_{186}$
participants received visual feedback about their actions as the pucks were shown $_{187}$
gliding on the surface from the initial position to the final position depending on the $_{188}$
exerted impulse. Thus, because the distances traveled by the two pucks for different $_{189}$
initial positions as a function of the button press-times t^{pre} could be observed, $_{190}$
participants could potentially use this feedback to adjust their press-times on $_{191}$
subsequent trials. Half the participants were randomly assigned to the 'light-to-heavy' $_{192}$
condition, in which the two pucks had masses of 1.5 kg and 2.0 kg, and the other half of $_{193}$
the participants were assigned to the 'heavy-to-light' condition, in which the pucks had $_{194}$
masses of 2.0 kg and 2.5 kg. $_{195}$

Phase 3: No feedback. In phase three, we wanted to investigate how having $_{196}$
observed the sliding of the pucks in phase two influenced participants' press-times with $_{197}$
an unknown puck. Subjects were asked to shoot a new puck they had not seen before to $_{198}$
the target without visual feedback, as in the first experimental phase (Fig. 1 B, *No* $_{199}$
Feedback). The texture of the puck consisted of five concentric rings. For participants in $_{200}$
the 'light-to-heavy' condition, the new puck had a mass of 2.5 kg whereas for $_{201}$
participants in the 'heavy-to-light' condition the new puck had a mass of 1.5 kg. $_{202}$
However, different from phase one, in which subjects had not obtained feedback about $_{203}$
the pucks' motion, by phase three participants had already interacted with three pucks $_{204}$
and obtained visual feedback about the motion of two pucks. Importantly, participants $_{205}$
had received feedback about the non-linear nature of gliding under friction in phase two. $_{206}$
Thus, this experimental phase allowed investigating, whether subjects use the functional $_{207}$
mapping from puck distances to press-times prescribed by Newtonian physics and what $_{208}$
assumptions about the mass of an unknown puck they used. $_{209}$

Phase 4: Collisions & no feedback. With the final experimental phase we wanted $_{210}$
to investigate, whether participants can use the relative mass ratios inferred from $_{211}$
observing collisions between two pucks to adjust their subsequent actions with one of $_{212}$
those pucks. At the beginning of phase four, participants watched a movie of $_{213}$
twenty-four collisions between two pucks. One was always the puck with unknown mass $_{214}$
used in phase three (without feedback; five rings) (see Fig. 1 B, *Collisions No* $_{215}$

Feedback), while the second puck was one of the two pucks presented in phase two (see Fig. 1 B, *Feedback*). Each collision thus showed one of the two previously seen pucks from phase two selected at random colliding with the puck from phase three with a total of twelve collision with each of the two known puck. By observing these elastic collisions participants were expected to learn the mass ratios between pucks, as shown in previous research [9,14]. Note that the pucks were simulated without the influence of friction in these collisions, ensuring that participants never observed the unknown puck gliding under the influence of friction. After watching these collisions, subjects were asked to shoot the puck from phase three again without obtaining visual feedback as in phases one and three. Thus, subjects interacted with the same puck as in phase three but had now seen the collisions of this puck with pucks they had interacted with. This experimental phase therefore allowed investigating, whether subjects used the learned mass ratios and transferred them to the control task to adjust their press-times. Importantly, having learned the mass ratios between pucks needs to be transferred to the press-times, which differ in a physically lawful way depending on the initial distance of the pucks to the target. Thus, if subjects used an internal model of physical relationships, they should be able to adjust their press-times for the new puck without ever having seen it glide.
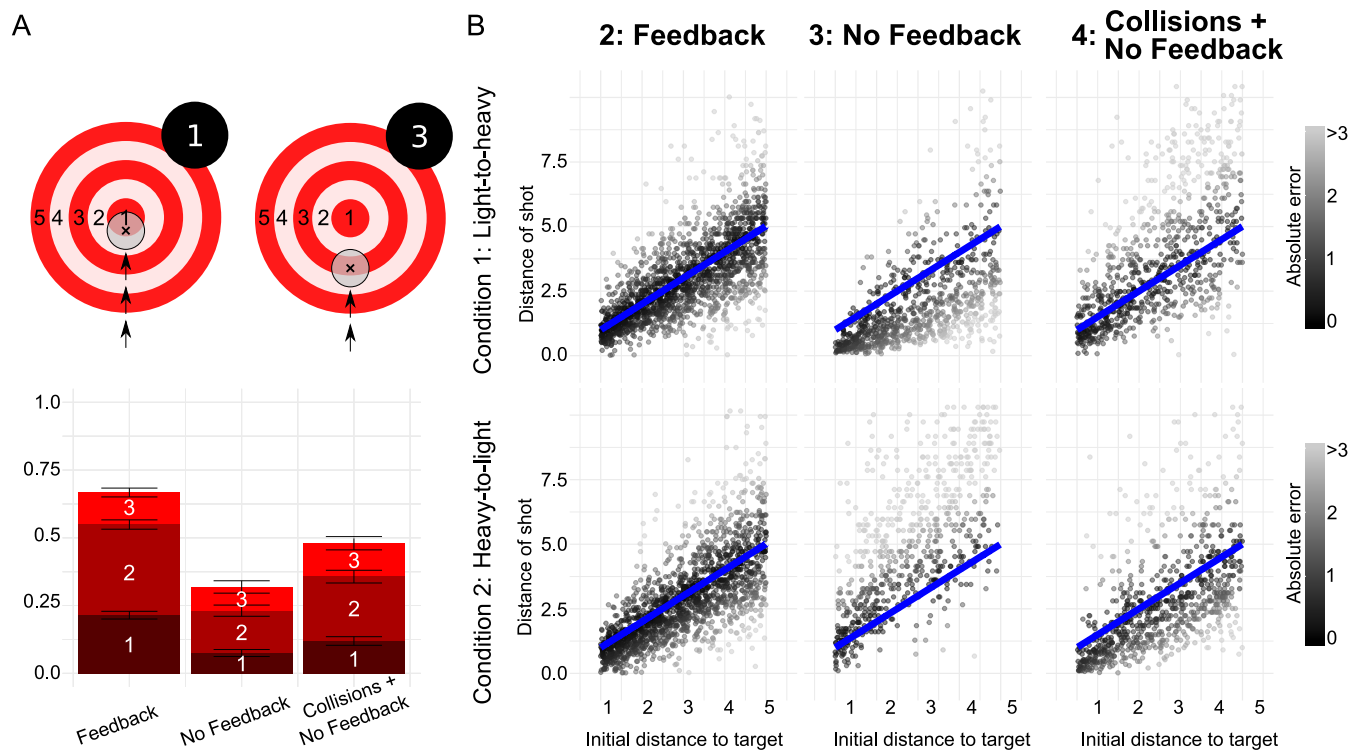
Results

Behavioral results

Fig 2. Task performance and pucks' traveled distance for three phases of experiment. **(A)** Participants' performance by experimental phase as quantified by pucks' average absolute error in final position. **(B)** Aggregated final positions of pucks versus initial distance of pucks to target. Phases of the experiment are separated by columns and conditions are separated by rows. The line of equality representing final positions prescribed by the Newtonian model with perfect knowledge of all parameters is shown in blue.

As subjects did not receive visual feedback about the consequences of their button $_{236}$
presses in the first phase of the experiment, the button press-times reflect the prior $_{237}$
assumptions they brought to the experiment. Indeed, subjects' press-times t^{pre} grew $_{238}$
with the initial distance between the puck and the target. The correlation between t^{pre} $_{239}$
and the initial distance was 0.482 ($p < 0.001$). However, the functional relationship $_{240}$
according to Newtonian physics prescribes a scaling of the press-time according to the $_{241}$
square-root of the distance as specified in eq. 1. The correlation between press-times $_{242}$
t^{pre} and the square-root of the initial distance was 0.478 ($p < 0.001$). We expected the $_{243}$
standard deviation of press-times to scale with the the mean of press-times in $_{244}$
accordance with the Weber-Fechner scaling. This was confirmed by subdividing the $_{245}$
range of distances into three intervals of the same size, i.e. $[1, 2.33]m$, $(2.33, 3.66]m$, and $_{246}$
$(3.66, 5]m$ and computing the standard deviation of press-times within these three $_{247}$
intervals resulting $2.97 \times 10^{-1}s$, $4.19 \times 10^{-1}s$, and $5.69 \times 10^{-1}s$. $_{248}$

In phase two, participants adjusted their press-times based on observing the gliding $_{249}$
of the pucks after button presses. Performance was evaluated by calculating the mean $_{250}$
absolute distance of pucks to the target after sliding. The mean absolute error over the $_{251}$
entire phase was $0.928m$ ($0.0177m$ SEM). Accordingly, the correlation between t^{pre} and $_{252}$
the initial distance was 0.644 ($p < 0.001$) and with the square-root of distance 0.646 $_{253}$
($p < 0.001$). The performance improved between the first eight trials at the beginning of $_{254}$
the phase (mean absolute error $1.76m$) and the last eight trials at the end of the phase $_{255}$
(mean absolute error $0.89m$). The adjustment of pressing times was achieved on average $_{256}$
after only a few trials, as revealed by a change-point analysis [27], which showed that $_{257}$
after six trials the average endpoint error of the puck was stable (see S1 Appendix, $_{258}$
"Change point detection"). Note that this includes four trials with one puck of the same $_{259}$
mass and two trials of the second puck with a different mass. $_{260}$

Phase three involved shooting a new puck, which subjects had previously not $_{261}$
interacted with, without visual feedback. Note that the puck was identical to the puck $_{262}$
subjects later interacted with in phase four after seeing the collisions. This phase $_{263}$
therefore allowed testing whether subjects used the non-linear scaling of the press-times $_{264}$
depending on initial distance of the puck after having observed the pucks' motion in $_{265}$
phase two. As expected, performance was significantly lower with the new puck without $_{266}$
obtaining visual feedback. Mean absolute error was $2.87m$ ($0.104m$ SEM). The $_{267}$
correlation between t^{pre} and the initial distance was 0.599 ($p < 0.001$) while the $_{268}$
correlation between t^{pre} and the square-root of the initial distance was 0.603 ($p < 0.001$). $_{269}$
Given that subjects had already obtained feedback about two pucks in phase two but $_{270}$
did not obtain feedback in this phase, their press-time distribution could potentially be $_{271}$
the mixture of the two press-time distributions of the two previous pucks, which were $_{272}$
different in the conditions 'light-to-heavy' and 'heavy-to-light'. We compared the $_{273}$
combined press-time distributions of phase two with the press-time distribution of phase $_{274}$
three for each condition with the Kolmogorov-Smirnov test. Press-times in phase three $_{275}$
reflected the behavior of both previous pucks combined for condition 'heavy-to-light' $_{276}$
(Kolmogorov-Smirnov, D = 0.0538, p = 0.092, see S1 Appendix, "Kolmogorov tests - $_{277}$
press-times in phase two & phase three") and approximately for condition $_{278}$
'light-to-heavy' (Kolmogorov-Smirnov, D = 0.156, $p < 0.001$, see S1 Appendix, $_{279}$
"Kolmogorov tests - press-times in phase two & phase three"). $_{280}$

At the beginning of phase four subjects watched a movie showing 24 collisions $_{281}$
between the pucks from phase two, for which visual feedback of the gliding had been $_{282}$
available, and the unknown puck from phase three. Thus, this condition allowed testing $_{283}$
whether observation of the collisions was used to infer the mass ratios of pucks and to $_{284}$
subsequently adjust the pressing times for that puck from phase three. Performance was $_{285}$
significantly higher than in phase three with a mean absolute error of $1.63m$ ($0.0440m$ $_{286}$
SEM), although the puck was the same as in phase three and although subjects did not $_{287}$
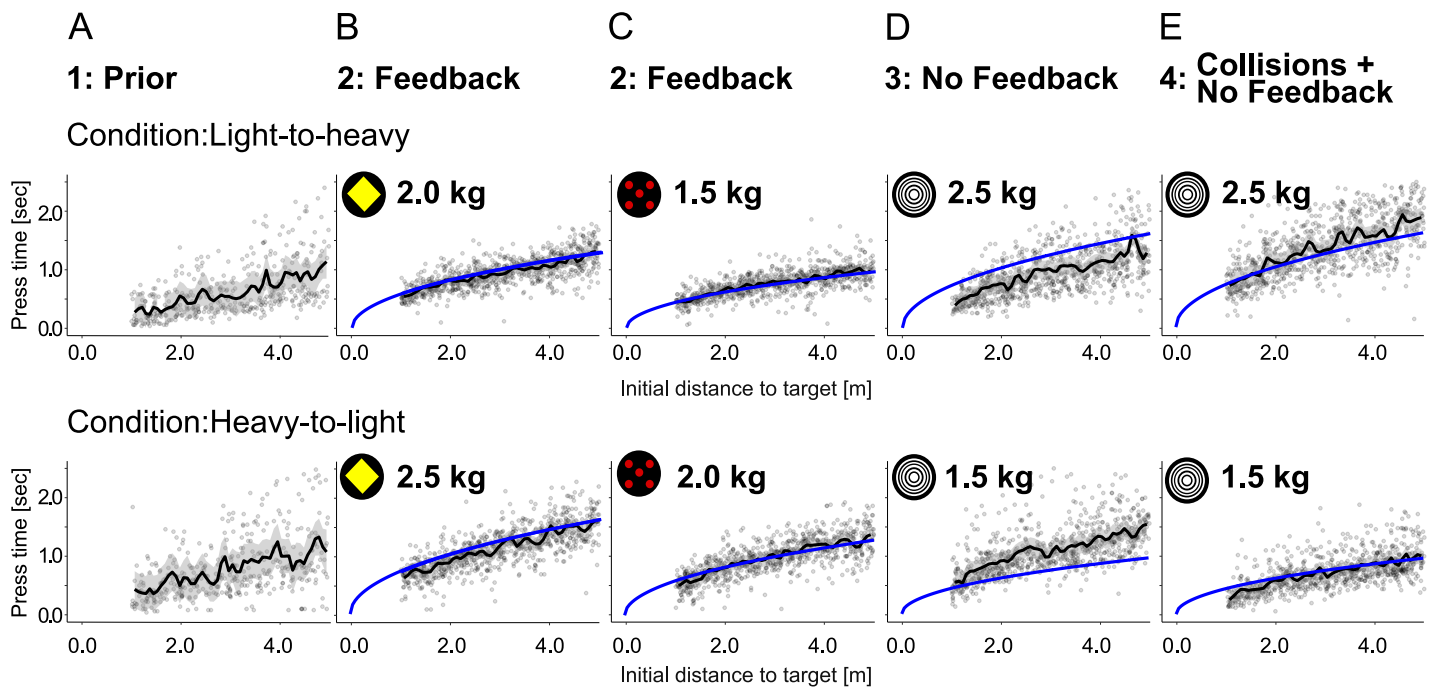
Fig 3. Press-times as function of initial distance to target. Press-times for all participants by condition and experimental phase are shown with data points in black and Newtonian relationship with perfect knowledge about the involved parameters in blue. The top row shows the data of subjects in the light-to-heavy condition and the bottom row shows the data of subjects in the heavy-to-light condition. **(A)** Press-times of participants in the first phase ("prior"), **(B)** second phase ("feedback") for the yellow puck, **(C)** second phase ("feedback") for the red puck, **(D)** third phase ("no feedback"), and **(E)** last phase ("collisions and no feedback") after having seen 24 collisions.

obtain visual feedback. This effect was significant for both conditions as tested with Wilcoxon Signed Rank test for the absolute error (light-to-heavy: W = 339300, p = 0.018; heavy-to-light: W = 441330, p < 0.001). This shift towards longer and shorter press-times in the light-to-heavy and heavy-to-light condition respectively is depicted in S1 Appendix, "Press-time distributions". The shift was statistically significant by testing with a Wilcoxon Signed Rank test for shorter and longer press-times for both conditions respectively (light-to-heavy: W = 158580, p < 0.001; heavy-to-light: W = 490620, p < 0.001). For more detail of the error distributions across phases two to four see S1 Appendix, "Distance error distributions".

Taken together, these analyses suggest, that subjects adjusted their press-times both depending on the distance of the pucks to the target and depending on the pucks' masses used in the simulation. Furthermore, the analyses provide initial evidence, that subjects scaled their press-times with a linear function of mass and with a square-root function of initial distance after having obtained visual feedback about the pucks' motion. Finally, observing collisions between pucks lead subjects to adjust their press-times even without obtaining visual feedback.

Model results

The above analyses give a first indication that our participants were able to adjust their press-times in accordance with Newtonian physics and that they transferred the inferences about relative mass ratios from observing collisions to the press-times. Nevertheless, the above analyses are limited in several ways. First, perceptual variables such as the initial distance of the puck to the target were uncertain for our subjects,

which is not quantitatively entering the correlation analyses of press times with physical   310
predictions under the assumption of perfect knowledge of all parameters. Secondly, our   311
participants had to press a button to propel the puck. For longer press-times, subjects   312
are known to demonstrate variability in pressing times, which scales linearly with its   313
mean and which may vary considerably between subjects. Thirdly, while subjects   314
pressed a button and observed the simulated motion of the pucks from a bird's eye view   315
on a monitor, it would be desirable to be able to estimate subjects' belief about the   316
masses of the different pucks implicit in their press-times. Therefore, we devised a   317
hierarchical Bayesian model of the full visuomotor decision task to provide a   318
computational account of our subject's behavior.

$\sigma^x = 0.05$

$x_{i,j}^{per} \sim Log\text{-}N(x_{i,j}, \sigma^{dist})$

$m_{j,k} \sim \Gamma(6, 2.5)$

$t_{i,j,k}^{int} = f(x_{i,j}^{per}, m_{j,k})$

$\sigma_j^t \sim \Gamma(1.2, 5)$

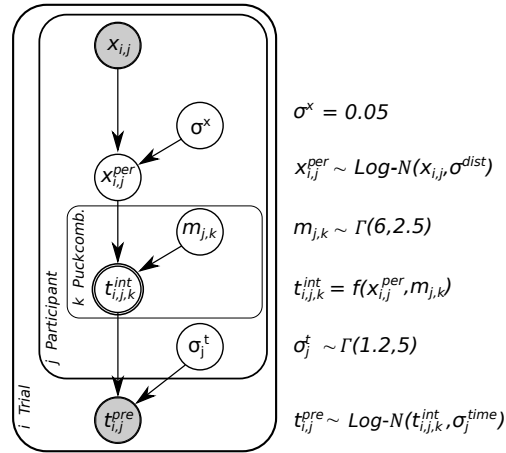$t_{i,j}^{pre} \sim Log\text{-}N(t_{i,j,k}^{int}, \sigma_j^{time})$

Fig 4. Hierarchical Bayesian network for the Newtonian model class. The model expresses the generative process of observed press-times $t_{i,j}^{pre}$ across trials i, participants j, and pucks k including Weber-Fechner scaling given perceptual uncertainties of distance $x_{i,j}$ and mass $m_{j,k}$ of the pucks and subjects' press-time variability. See the text for details.

                                                                                                                    319
The Bayesian network model in Fig. 4 expresses the relationship between variables   320
on a subject-by-subject and trial-by-trial basis. While as experimenters we have access   321
to the true initial distance x used in the simulation of the puck and displayed on the   322
monitor as well as the measured press-time t^{pre} chosen by the subject on a particular   323
trial i, subjects themselves do not know these values. Instead, each participant j has   324
some uncertain percept of the puck's distance $x_{i,j}^{per}$ and, potentially, some belief about   325
the mass $m_{j,k}$ of the puck, which depends on its color and the phase of the experiment   326
k. This structure of the graphical model from the experimenter's view leads to the   327
following joint distribution $p(d, l)$ with observed data $d = \{x, t^{pre}\}$ and latent variables   328
$l = \{x^{per}, \sigma^x, m, \sigma^t\}$, where trial, puck and participant subscripts were omitted for   329
clarity: 330

$$p(d, l) = p(x) \ p(\sigma^x) \ p(x^{per}|x, \sigma^x) \ p(m) \ p(\sigma^t) \ p(t^{pre}|x^{per}, m, \sigma^t, \theta) \qquad (2)$$

Here, $p(x)$ is known to the experimenter as the actual distribution of distances to target   331
used in the simulations. By contrast, the distribution of perceived distances   332
$p(x^{per}|x, \sigma^x)$ is the noisy perceptual measurement by our participants described as a   333
log-normal distributed variable, ensuring that samples are strictly positive and including   334
uncertainty scaling according to Weber-Fechner [28]. $p(\sigma_x)$ describes the prior   335
distribution over possible values of this perceptual uncertainty. Participants' prior   336
beliefs about the masses of the different pucks $p(m)$ are described by gamma   337
distributions, which entail the constraint that masses have to be strictly positive. The   338
log-normal distribution of actually measured press-times $p(t^{pre}|x^{per}, m, \sigma^t)$ depends on   339

the noisy perception of the distance to target x^{per}, the belief about the mass of the object and the variability in acting, which is the press-time variability σ^t with its' gamma distribution $p(\sigma^t)$. We additionally summarize all constant factors, i.e the surface friction coefficient, the gravitational acceleration, the constant interaction force in the parameter θ.

The potential functional relationship between the perceived distance of the puck to the target and the required press-time is expressed in the deterministic node representing t^{int} in the Bayesian network. We consider two possible functional relationships between the press-time and the distance to be covered: subjects may use a linear relationship between press-time and initial distance as a simple heuristic approach:

$$H_1 : \quad \mathrm{t}^{\mathrm{int}} \propto \mathrm{x}^{\mathrm{per}} \tag{3}$$

or may use the square-root relationship as prescribed by Newtonian physics according to Eq. 1:

$$H_2 : \quad \mathrm{t}^{\mathrm{int}} \propto \sqrt{\mathrm{x}^{\mathrm{per}}} \tag{4}$$

As experimenters, we only have access to the observed data d, i.e. the actual distances given the experimental setup and the measured press-times. We use Bayesian inference employing Markov-Chain Monte-Carlo to invert the generative model and infer the latent variables describing subjects' internal beliefs given the observed data d:

$$p(l|d) = \frac{p(d,l)}{p(d)} = \frac{p(\sigma^x)\ p(x^{per}|x,\sigma^x)\ p(m)\ p(\sigma^t)\ p(t|x^{per},m,\sigma^t,\theta)}{p(t|x)} \tag{5}$$

However, modeling perception as inference may not be sufficient to describe our participants' behavior and their selection of actions. In order to include this selection we take potential cost functions into account. Cost functions govern which action from an action space, here the possible press-times, is considered to best suit the demands of the task. This means that it is assumed that participants select an action that minimizes potential costs associated with missing the target. Loss functions, describing the rewards or costs for every action in the action space, can have any arbitrary form, nonetheless we chose a set of three standard loss functions and compare their predictions: 0-1, absolute and quadratic loss functions. It can be shown that these loss functions lead to different decisions for a continuous variable with a non-symmetric distribution [29]. Thus, assuming that humans do have costs for missing the target and associated policies to minimize these costs, leads to three different model versions for each model class (see S1 Appendix, "Implementation of cost functions").

In order to evaluate participants' behavior computationally we first utilized subjects' data from phase two of the experiment to estimate their perceptual uncertainty and behavioral variability. We chose to start with analyzing phase two for two reasons: first, if participants are able to use visual feedback about the pucks' dynamics to adjust their press-times, predictions of the model with the correct physical relationships should capture the behavior better than the linear heuristics model. Secondly, inferred values for latent variables describing visual uncertainty in distance estimation and variability in press-times are less prone to be assigned additional uncertainty. Additional uncertainty arising in all other phases of the experiment due to the lack of visual feedback should be assigned to the uncertainty about the mass or the linear scaling rather than to the variability of press-times in general. Therefore, by evaluating data from phase two "feedback" first, values for the press-time variability and uncertainty in the perception of distances can be estimated for each participant.

First, we used the data of phase two "feedback" to investigate, which of the three loss functions best describes our participants' data. In order to choose the appropriate
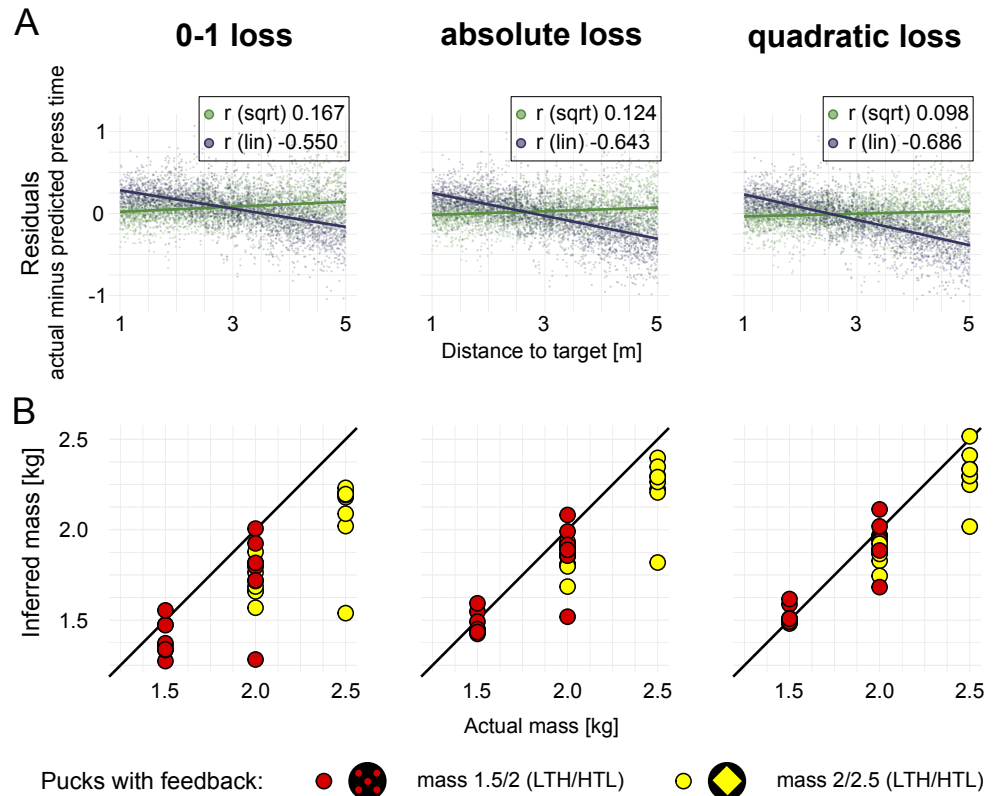
Fig 5. Residuals of estimated press times and inferred masses in phase two for three cost functions. (**A**)Residuals were calculated for each participant and each puck in phase two ("feedback") given the actual press-times and the best fits for the linear heuristics and the Newtonian model. Residuals for both models were calculated for all three cost functions. (**B**) MAP estimates of the masses used by individual subjects inferred according to the Newtonian model for the the three cost functions. Red and yellow pucks had different masses for subjects in the two conditions "heavy-to-light" and "light-to-heavy".

cost function explaining participants' actions most accurately, we computed the press-times predicted by the linear heuristics and the Newtonian model and applied the three cost functions to both models. This was achieved by using the inferred maximum a posteriori (MAP) values for the latent variables in both model classes, i.e. the mass m in the Newtonian and a linear factor in the heuristic linear model class. This allowed calculating the residuals, i.e. the difference between subjects' actual press-times and the predicted press-times for all six combinations of two models and three cost functions. The residuals are shown as a function of the distance to the target in Fig.5. The strong correlation of residuals and distance to target indicates a systematic bias of the linear heuristics model, whereas the weak correlation of the Newtonian model demonstrates its superiority in explaining the measured data. These relationships were tested with Spearman correlation tests for each model and cost function. Showing highly significant correlations for each test (p < 0.001) and higher correlation in the linear model for each cost function (0-1 loss function: $\rho_{New} = 0.167$, $\rho_{lin} = -0.550$; abs. loss function: $\rho_{New} = 0.124$, $\rho_{lin} = -0.643$; quadratic loss function: $\rho_{New} = 0.0976$, $\rho_{lin} = -0.686$). Thus, with respect to cost functions the Newtonian model with quadratic cost shows the lowest residual correlation, which from here on will be used as the proposed cost function for both model classes.

Secondly, a further indication, that the Newtonian model together with the

quadratic cost function better described the data was obtained by comparing posterior   404
mass beliefs inferred separately for each cost function. Posterior distributions inferred   405
with data aggregated over participants only from phase two match actual masses   406
implemented in the physical simulations better for the quadratic cost function (see S1   407
Appendix, "Latent masses by cost function: aggregated data from phase 'feedback'").   408
In both conditions inferred beliefs about the masses are closer to the actual masses   409
implemented in the simulations when presuming that participants use a quadratic loss   410
function. This was confirmed by testing for the absolute differences between the   411
posterior belief and the actual mass for each condition, puck and cost function. ANOVA   412
revealed highly significant differences (F = 486, p < 0.001) and post-hoc tests showed   413
that the posterior belief when using the quadratic cost function is the closest fit for all   414
pucks (p < 0.001 condition light-to-heavy, yellow diamond puck; p = 0.002 red dots   415
puck; p < 0.001 condition heavy-to-light, yellow diamond puck; p < 0.001 red dots   416
puck). This result also held at the individual participant levels as illustrated in Fig.5   417
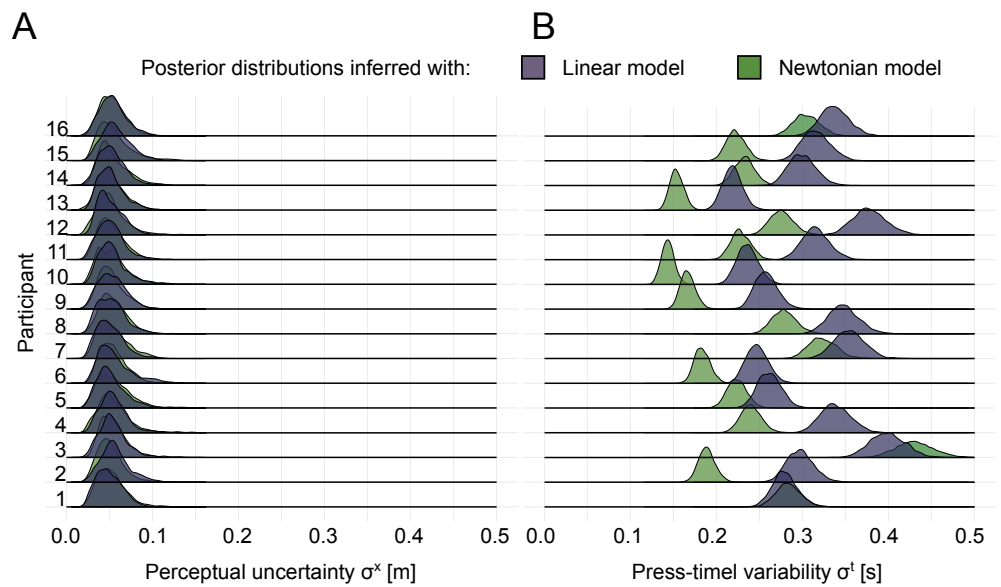(B)).   418

Fig 6. Posterior estimates of perceptual uncertainty and press-time variability inferred with data from phase two "feedback". **(A)** Inferred posterior distributions of perceptual uncertainty for the linear heuristics model and the Newtonian physics model. Dark green distributions display posterior distributions for the Newtonian model class, dark blue ones for the linear model class. A separation into cost functions is not included since the different cost functions did not lead to significant differences. **(B)** Inferred posteriors for individual press-time variability varied significantly between subjects between the two models. All but one participant show lower or equal values of variability regarding the press-time for the Newtonian model class.

Finally, the posterior predictive distributions for press-times estimated from data in   419
phase two (see S1 Appendix, "Posterior predictive checks for press-times") match the   420
actual behavior of the participants more closely compared to the linear heuristics model.   421
Kullback-Leibler divergence for each pair support this with divergence values at 0.0558   422
and 0.0851 for the Newtonian and linear model, respectively. Not only did the   423
Newtonian model capture participants' press-times in phase two better than the linear   424
heuristics model, but this also affected the inferred variabilities. While perceptual   425
uncertainty only varied marginally (see Fig.6 (A)), the posterior distributions of the   426
press-time variability σ_j^t show higher values for the linear model (see Fig.6 (B))   427

compared to the Newtonian model. This was confirmed by calculating a repeated measure ANOVA on the posterior distributions of press-time variability for both models, showing that the difference was highly significant (F = 39.2, p < 0.001). This elevated level of uncertainty is necessary for the linear heuristics model to compensate for the diminished ability to capture the relationship of initial distances and participants' press-times.
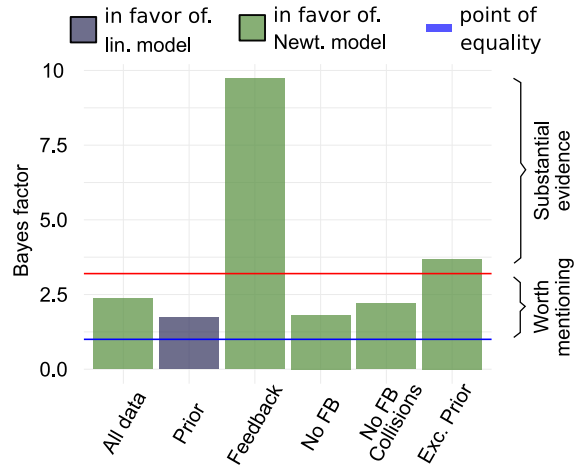

Fig 7. Bayes factors calculated from posterior odds sampled using the product space method. Bayes factors are displayed for different phases and combinations of phases. Blue line at 1 marks the point where neither model is stronger supported by evidence. Red line at 3.2 marks the transition from Bayes factors being only worth mentioning to substantial evidence in favor of one the models. Colors of bars indicate the model favored by the Bayes factors.

Subsequently, we used the MAP values of the inferred press-time variabilities $\hat{\sigma}^t_{MAP}$ for each subject as fixed values for the analyses of data of all experimental phases. The same applied for the MAP values of the inferred perceptual uncertainties $\hat{\sigma}^x_{MAP}$ which did not differ across subjects or models (see Fig.6 (A)) and therefore were set to one fixed value for all subjects. Note that the mean was $0.05m$ in simulation space, which, given the current setup corresponded to approximately 1.8 pixels on the monitor. Using the hierarchical Bayesian model, samples of the posterior predictive distributions of press-times and of the perceptual uncertainty are used to infer latent variables for both the linear and the Newtonian models. The posterior predictive distributions of press-times are shown in the S1 Appendix, "Posterior predictive checks for press-times in both models". Evidence was in favor of the Newtonian model compared to the heuristics model across all phases of the experiment with the exception of the *Prior* phase. The largest differences in prediction power appears in the *Feedback* phase with the Newtonian model being the considerably better choice to describe the actual press-times. This superiority of the Newtonian model over the linear heuristic one remains in the subsequent phases even without any visual feedback. This was again tested by running two-sample Kolmogorov-Smirnov tests for posterior predictive distributions of phase three of both models and the actual data, as well as calculating the Kullback-Leibler divergence for each pair. Resulting in lower K-S statistic values for the Newtonian model (D = 0.0436, p = 0.00521) compared to the linear one (D = 0.0851, p < 0.001). KL divergence values are 0.0582 and 0.0599 for the Newtonian and linear model, respectively.

Finally, to confirm that the behavioral data of our subjects was best described by the Newtonian model with quadratic cost function we carried out model selection using

the *product space method* [30]. In this approach, a mixture model combines both the $\qquad$ 458
linear and the Newtonian model to account for the data. An index variable indicates, $\qquad$ 459
which of the two models is selected at each iteration to explain the data. Given that $\qquad$ 460
both models have the same a priori probability to be chosen, the Bayes factor equates $\qquad$ 461
to the posterior odds of the index variable. Resulting Bayes factors are shown in Fig.7. $\qquad$ 462
Given the complete data set from all phases there is small support for the Newtonian $\qquad$ 463
model (Bayes factor K of 2.33). When only considering data from the *Prior* phase there $\qquad$ 464
is weak support for the linear model ($K = 1.88$). Instead, when considering all phases $\qquad$ 465
but the first phase there is substantial support for the Newtonian model ($K = 3.71$) $\qquad$ 466
and strong evidence for the square-root model in the feedback phase ($K = 9.71$).
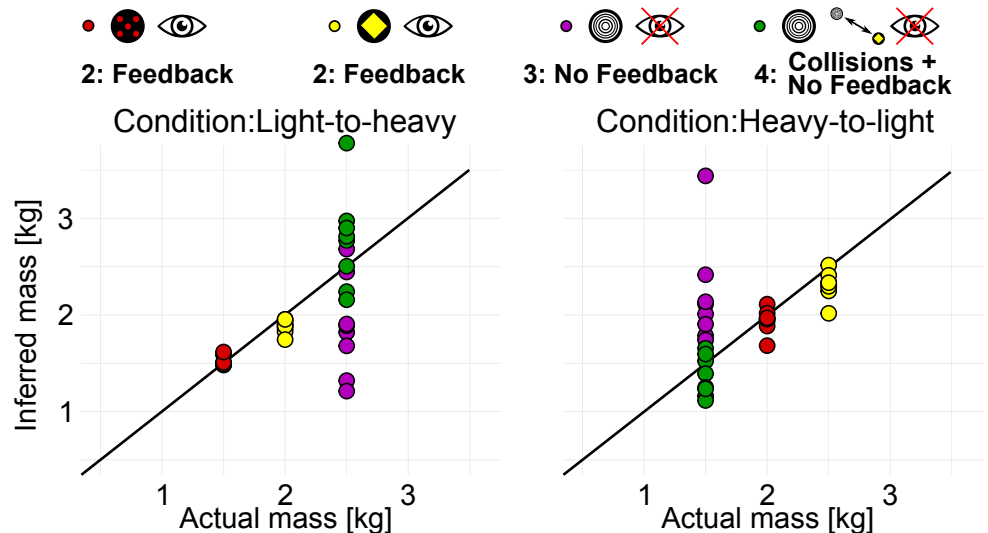
Fig 8. MAP values of inferred latent mass in Newtonian model class with quadratic loss function for each participant and condition.

467

The hierarchical Bayesian model also allows inferring the masses best describing our $\qquad$ 468
subjects' internal beliefs given the Newtonian model and the measured press-times. Not $\qquad$ 469
surprisingly, mean mass beliefs vary strongly across subjects in the *Prior* phase, where $\qquad$ 470
participants had to make decisions without any observations of the pucks, only relying $\qquad$ 471
on their prior beliefs about the potentially underlying dynamics and environmental $\qquad$ 472
conditions (see S1 Appendix "Latent masses: phase 'prior' and 'feedback'" for gray $\qquad$ 473
posterior distributions). Nevertheless, the variances of mass beliefs within the first $\qquad$ 474
phase were surprisingly small for individual subjects with a mean of 0.0023 kg, $\qquad$ 475
potentially indicating that each subject consistently used a belief about the mass of the $\qquad$ 476
puck. Inferred values for these prior mass beliefs are displayed in the Appendix S1 $\qquad$ 477
"Latent masses: phase prior and feedback" for each participant. When obtaining visual $\qquad$ 478
feedback in the *Feedback* phase of the experiment, subjects only needed on average six $\qquad$ 479
trials to adjust their press-times so that mass beliefs were stable thereafter. Implicit $\qquad$ 480
mass beliefs were quite accurate with the mean of inferred MAP values at 1.5218 and $\qquad$ 481
1.8818 kg in the condition light-to-heavy (1.5 and 2.0 kg) and 1.9415 and 2.3068 kg in $\qquad$ 482
condition heavy-to-light (2.0 and 2.5 kg). Fig. 8 shows the MAP estimates of the $\qquad$ 483
masses for both conditions and phases two to four for all subjects. $\qquad$ 484

In phase three *No Feedback* participants faced an unknown puck without any visual $\qquad$ 485
feedback but with the acquired knowledge about the relationship of press-time and $\qquad$ 486
distance. Thus, participants had to select press-times without knowing the mass of the $\qquad$ 487
unknown puck. As reported above, the press-time distributions in this phase of the $\qquad$ 488
experiment were close to the combined press-times that subjects had used for the two $\qquad$ 489

pucks in the previous phase two of the experiment. The corresponding MAP mass beliefs were accordingly approximately the average of the two previous pucks' masses with 1.87 and 2.19kg and corresponding mass distributions differed significantly for the two conditions light-to-heavy and heavy-to-light (ANOVA: F = 1060, p < 0.001; see also S1 Appendix, "Latent masses: phase "no feedback" and "collision and no feedback""). But after observing the 24 collisions in phase *Collisions + No Feedback* of the two known pucks with the unknown puck participants were able to adjust their press-times so that the estimated mass beliefs were significantly closer to the true values used in the simulations than in the previous phase. This was quantified by running a repeated measures ANOVA of the deviations from the actual mass (F = 7.103, p = 0.0176). Thus, the mass beliefs implicit in our participants' press-times reflected the inferred mass ratios and transferred from having observed the pucks' collisions to the subsequent visuomotor control task.

Discussion

Although people are able to interact with the physical world successfully in every-day activities, classic research has contended that human physical reasoning is fundamentally flawed [1–4]. Recent studies instead have shown that biased human behavior in a range of perceptual judgement tasks involving physical scenarios can be well described when taking prior beliefs and perceptual uncertainties into account [9–12]. The reason is that, inferences in general need to integrate uncertain and ambiguous sensory data and partial information about object properties with prior beliefs [5–8]. Much less is known about how intuitive physical reasoning guides actions. Here, we used a perceptual inference task involving reasoning about relative masses of objects from the intuitive physics literature and integrated it with a visuomotor task. Subjects had to propel a simulated puck into a target area with a button press whose duration was proportional to the puck's release velocity. The goal was to investigate how people utilize relative masses inferred from watching object collisions to guide subsequent actions.

Specifically, we devised an experiment consisting of four phases, which differed in the available sensory feedback and prior knowledge about objects' masses available to participants. The physical relationship underlying the task requires subjects to press a button for a duration that is proportional to the mass of the puck and proportional to the square-root of the initial distance. This allowed examining peoples' prior assumptions about the underlying dynamics of pucks' gliding, their ability to adjust to the pucks' initial distances to the target and to the varying masses of pucks, and the transfer of knowledge about relevant properties gained by observing collisions between pucks. Using a hierarchical Bayesian model of the control task accommodating individual differences between subjects and trial by trial variability allowed analyzing subjects' press-times quantitatively.

In the prior phase without visual feedback, subjects adjusted their press-times with the initial distance of the puck to the target. Not surprisingly, because subjects did not obtain any feedback about their actions and therefore the degree of friction, the magnitude of the applied force, and the scale of the visual scene, could only hit the target by chance. Nevertheless, model selection slightly favored the linear heuristics model compared to the square-root model, i.e. subjects approximately scaled the press-times linearly with the initial distance to target. Thus, subjects came to the experiment with the prior belief that longer press-times would result in longer sliding distances but did not scale their press-times according to the square-root of the initial distance of the pucks as prescribed by Newtonian physics. As subjects did not sense the weight of the pucks and did not obtain any visual feedback about the pucks' motion, the observed behavior in this phase of the experiment may be dominated by the uncertainty

about the underlying mapping between the duration of button presses and the pucks' $\quad$ 540
release velocities, the effects of friction, and the visual scale of the simulation. $\quad$ 541

When visual feedback about the pucks' motion during the feedback phase was $\quad$ 542
available, subjects needed on average only six trials to reach stable performance. This is $\quad$ 543
particularly remarkable, because it corresponds to adjusting the press-times to a single $\quad$ 544
puck's mass over the four initial trials and then adjusting the press-times within only $\quad$ 545
two subsequent trials to a new puck with a different mass. Thus, the observation of the $\quad$ 546
pucks' dynamics over six trials was sufficient to adjust the press-times with the $\quad$ 547
square-root of initial distance and linearly with the mass, which was by itself not $\quad$ 548
observable. Data from this phase of the experiment were utilized to infer parameters $\quad$ 549
describing individual subjects' perceptual uncertainty and motor variability. Perceptual $\quad$ 550
variability was consistent across subjects and varied only marginally so that a constant $\quad$ 551
value of $\sigma^x = 0.05m$ was used across subjects and models for all other phases of the $\quad$ 552
experiment. Remarkably, this corresponds to a distance of pixels in the horizontal $\quad$ 553
direction on the display monitor with a resolution of 1080 pixels. By contrast, the $\quad$ 554
variability of press-times σ^t varied substantially across subjects with almost all subjects $\quad$ 555
lying between $0.15s$ and $0.33s$, so that individuals' parameters were used in all $\quad$ 556
subsequent models. $\quad$ 557

Given that the variability of peoples' press-times scales with the mean of the $\quad$ 558
duration, longer press-times can lead to larger deviations from the targeted press-time. $\quad$ 559
To reduce possible overshoots, participants may implicitly use a cost function $\quad$ 560
quantifying the relative desirability of the pucks' final distance to the target. Therefore, $\quad$ 561
we tested which of three commonly used cost functions best described subjects' $\quad$ 562
press-times: the 0-1 cost function, the quadratic cost function, and the absolute value $\quad$ 563
cost function. Using these three cost functions together with the hierarchical Bayesian $\quad$ 564
model, we analyzed the correlation of the residuals between predicted and observed $\quad$ 565
press-times with the initial distance to target. For each cost function, the Newtonian $\quad$ 566
square-root model showed smaller Spearman correlations, and overall, the smallest $\quad$ 567
correlation of $\rho_{New} = 0.0976$ was achieved by the square-root model and the quadratic $\quad$ 568
cost functions. Thus, our subjects' press-times were best explained by a quadratic cost $\quad$ 569
function, which we used for the remaining analyses. $\quad$ 570

Model selection using the product space method showed that the press-times were $\quad$ 571
best explained by the Newtonian physics model when taking into account perceptual $\quad$ 572
uncertainty, motor variability and the quadratic cost function. Similarly, this was $\quad$ 573
confirmed through posterior predictive checks of press-times for the two models. Thus, $\quad$ 574
participants adjusted the press-times with the square-root of the initial distance to the $\quad$ 575
target and used the contextual color cue of the pucks to adjust the press-times. $\quad$ 576
Subjects only had the contextual cue of different colors between the two pucks but $\quad$ 577
adjusted the press-times in such a way that this was interpretable in terms of the two $\quad$ 578
different masses used in the puck's simulations. Therefore, just on the basis of these $\quad$ 579
adjustments alone, one might argue that subjects may have adjusted their press-times $\quad$ 580
based on the available visual feedback about the pucks' motion without any recurrence $\quad$ 581
to a the concept of physical mass. That this is unlikely, is due to the following two $\quad$ 582
phases of the experiment. $\quad$ 583

Previous research has demonstrated, that people can infer the mass ratios of objects $\quad$ 584
from observing their collisions [9,11,12] and that prior beliefs can be transferred between $\quad$ 585
distinct scenarios and tasks [31]. Here, subjects were asked to propel one particular $\quad$ 586
puck before and after seeing 24 collision between this puck and the two pucks for which $\quad$ 587
they had previously obtained visual feedback. Subjects utilized the inferred mass ratios $\quad$ 588
to adjust their press-times to reach the target more accurately. Model selection $\quad$ 589
provided evidence, that subjects continued to use the square-root relationship of initial $\quad$ 590
distance. Thus, subjects scaled their press-times according to Newtonian physics to $\quad$ 591

successfully propel the puck to the target. Note that beyond the color cue, subjects did not know the pucks' masses. While subjects assigned to the condition light-to-heavy had interacted with pucks with $1.5kg$ and $2.0kg$, subject in the heavy-to-light condition had interacted with pucks with $2.0kg$ and $2.5kg$. That the different dynamics were to attribute to different masses and that relative masses from observing the collisions could be transferred to press-times entirely relied on subjects intuitive physical reasoning. Thus, subjects utilized the relative masses inferred from observing pucks' collisions and transferred them to the puck shooting task according to Newtonian physics.

The hierarchical Bayesian model furthermore allowed inferring the latent variables describing our participants' behavior. First, the posterior means of press-time variability σ^t were smaller for the Newtonian model compared to the linear heuristics model for all but one subject. This reflects the fact that additional variability due to the weaker ability to model the relationship between initial distances and press-times needs to be accommodated by the linear model. Secondly, the posterior means of masses best explaining our participants' press-times were closer to the true masses used in the pucks' simulations for the quadratic cost function compared to the 0-1 and the absolute-value cost functions. Thus, while previous research has demonstrated that human biases and systematic deviations from the predictions of Newtonian physics are attributable to perceptual uncertainties and prior beliefs, the present experiments and analyses provide evidence that costs functions implicit in subjects' behavior also need to be taken into account for explaining such deviations.

Taken together, the present study is in accordance with previous studies on intuitive physics within the noisy Newton framework [13]. The systematic deviations in our subjects' press-times from the those prescribed by Newtonian physics under full knowledge of all parameters were explained quantitatively as stemming from perceptual uncertainties interacting with prior beliefs according to probabilistic reasoning. Previous studies had also shown, that people are able to infer relative masses of objects from their collisions [9, 11, 12]. The present study additionally shows, that subjects can utilize such inferences and transfer them to a subsequent visuomotor task. This establishes a connection between reasoning in intuitive physics [9–12] and visuomotor tasks [19, 21, 23, 25].

Crucial in the quantitative description of participants' behavior was the inclusion of a cost function. Commonly, cost functions in visuomotor behavior are employed to account for explicit external rewards imposed by the experimental design, e.g. through monetary rewards [19, 32] or account for costs associated with the biomechanics or accuracy of movements [21, 22]. The present model used a cost function to account for the costs and benefits implicit in our participants visuomotor behavior and may encompass external and internal cost related to different task components, perceptual, cognitive, biomechanical costs and preferences. Inferring such costs and benefits has been shown to be crucial for the understanding of visuomotor behavior [33–35]. Thus, participants' deviations from predictions of Newtonian physics were in part attributable to prior beliefs and perceptual uncertainties and in part by a cost function quantifying the internal costs for errors due to participants' internal variability.

The results of the present study furthermore support the notion of structured internal causal models comprising physical object representations and their dynamics. Although our participants never sensed the weight of pucks, they readily transferred their visual experiences by interpreting them in terms of the physical quantity of mass. A recent study [36] found support at the implementational level for representations of mass in parietal and frontal brain regions that generalized across variations in scenario, material, and friction. While our results do not provide direct evidence for the notion of internal simulations of a physics engine [37], they also do not contradict them. While it could be argued that structured recognition models may be sufficient for the inference

of object properties such as mass, in our experiment subjects had to act upon such inferences, which strongly suggest the availability of representations of mass.

Finally, the present study also shows the importance of using structured probabilistic generative models that contain interpretable variables when attempting to quantitatively reverse engineer human cognition [38]. Previous research has demonstrated pervasive and systematic deviations of human reasoning from probabilistic accounts [39]. Similarly, systematic deviations in physical reasoning [1–4] have been interpreted as failures of physical reasoning. It is only more recently, that these deviations have been explained through computational models [9–12, 37] involving structured generative models relating observed and latent variables probabilistically. These models involve the explicit modeling of prior beliefs and perceptual uncertainties [5, 6] as well as uncertainties in visuomotor behavior [19–21], which have been modeled successfully in a probabilistic framework. As such, the present study is in line with efforts of understanding perception and action under uncertainty through computational models, which use structured probabilistic generative models and external as well as internal costs [8].

References

1. McCloskey M, Caramazza A, Green B. Curvilinear motion in the absence of external forces: Naive beliefs about the motion of objects. Science. 1980;210(4474):1139–1141.

2. Todd JT, Warren Jr WH. Visual perception of relative mass in dynamic events. Perception. 1982;11(3):325–335.

3. Gilden DL, Proffitt DR. Heuristic judgment of mass ratio in two-body collisions. Perception & Psychophysics. 1994;56(6):708–720.

4. Cohen AL. Contributions of invariants, heuristics, and exemplars to the visual perception of relative mass. Journal of experimental psychology: human perception and performance. 2006;32(3):574.

5. Knill DC, Richards W. Perception as Bayesian inference. Cambridge University Press; 1996.

6. Kersten D, Mamassian P, Yuille A. Object perception as Bayesian inference. Annu Rev Psychol. 2004;55:271–304.

7. Griffiths TL, Chater N, Kemp C, Perfors A, Tenenbaum JB. Probabilistic models of cognition: Exploring representations and inductive biases. Trends in cognitive sciences. 2010;14(8):357–364.

8. Gershman SJ, Horvitz EJ, Tenenbaum JB. Computational rationality: A converging paradigm for intelligence in brains, minds, and machines. Science. 2015;349(6245):273–278.

9. Sanborn AN, Mansinghka VK, Griffiths TL. Reconciling intuitive physics and Newtonian mechanics for colliding objects. Psychological review. 2013;120(2):411.

10. Smith KA, Battaglia P, Vul E. Consistent physics underlying ballistic motion prediction. In: Proceedings of the Annual Meeting of the Cognitive Science Society. vol. 35; 2013.

11. Smith KA, Vul E. Sources of uncertainty in intuitive physics. Topics in cognitive science. 2013;5(1):185–199.

12. Hamrick JB, Battaglia PW, Griffiths TL, Tenenbaum JB. Inferring mass in complex scenes by mental simulation. Cognition. 2016;157:61–76.

13. Kubricht JR, Holyoak KJ, Lu H. Intuitive physics: Current research and controversies. Trends in cognitive sciences. 2017;21(10):749–759.

14. Smith KA, Dechter E, Tenenbaum JB, Vul E. Physical predictions over time. In: Proceedings of the annual meeting of the cognitive science society. vol. 35; 2013.

15. Smith KA, Battaglia PW, Vul E. Different physical intuitions exist between tasks, not domains. Computational Brain & Behavior. 2018;1(2):101–118.

16. Kaiser MK, Proffitt DR, Whelan SM, Hecht H. Influence of animation on dynamical judgments. Journal of experimental Psychology: Human Perception and performance. 1992;18(3):669.

17. Kaiser MK, Proffitt DR, McCloskey M. The development of beliefs about falling objects. Perception & Psychophysics. 1985;38(6):533–539.

18. McCloskey M, Kohl D. Naive physics: The curvilinear impetus principle and its role in interactions with moving objects. Journal of Experimental Psychology: Learning, Memory, and Cognition. 1983;9(1):146.

19. Trommershäuser J, Maloney LT, Landy MS. Statistical decision theory and the selection of rapid, goal-directed movements. JOSA A. 2003;20(7):1419–1433.

20. Körding KP, Wolpert DM. Bayesian integration in sensorimotor learning. Nature. 2004;427(6971):244.

21. Körding KP, Wolpert DM. Bayesian decision theory in sensorimotor control. Trends in cognitive sciences. 2006;10(7):319–326.

22. Todorov E. Optimality principles in sensorimotor control. Nature neuroscience. 2004;7(9):907–915.

23. Zago M, Bosco G, Maffei V, Iosa M, Ivanenko YP, Lacquaniti F. Internal models of target motion: expected dynamics overrides measured kinematics in timing manual interceptions. Journal of neurophysiology. 2004;91(4):1620–1634.

24. McIntyre J, Zago M, Berthoz A, Lacquaniti F. Does the brain model Newton's laws? Nature neuroscience. 2001;4(7):693.

25. Flanagan JR, Bittner JP, Johansson RS. Experience can change distinct size-weight priors engaged in lifting objects and judging their weights. Current Biology. 2008;18(22):1742–1747.

26. Baugh LA, Kao M, Johansson RS, Flanagan JR. Material evidence: Interaction of well-learned priors and sensorimotor memory when lifting objects. Journal of neurophysiology. 2012;108(5):1262–1269.

27. Lee MD, Wagenmakers EJ. Bayesian cognitive modeling: A practical course. Cambridge university press; 2014.

28. Battaglia PW, Kersten D, Schrater PR. How haptic size sensations improve distance perception. PLoS computational biology. 2011;7(6):e1002080.

29. Gelman A, Carlin JB, Stern HS, Dunson DB, Vehtari A, Rubin DB. Bayesian data analysis. Chapman and Hall/CRC; 2013.

30. Lodewyckx T, Kim W, Lee MD, Tuerlinckx F, Kuppens P, Wagenmakers EJ. A tutorial on Bayes factor estimation with the product space method. Journal of Mathematical Psychology. 2011;55(5):331–347.

31. Houlsby NM, Huszár F, Ghassemi MM, Orbán G, Wolpert DM, Lengyel M. Cognitive tomography reveals complex, task-independent mental representations. Current Biology. 2013;23(21):2169–2175.

32. Dayan P, Daw ND. Decision theory, reinforcement learning, and the brain. Cognitive, Affective, & Behavioral Neuroscience. 2008;8(4):429–453.

33. Hoppe D, Rothkopf CA. Learning rational temporal eye movement strategies. Proceedings of the National Academy of Sciences. 2016;113(29):8332–8337.

34. Zhang R, Zhang S, Tong MH, Cui Y, Rothkopf CA, Ballard DH, et al. Modeling sensory-motor decisions in natural behavior. PLoS computational biology. 2018;14(10):e1006518.

35. Hoppe D, Rothkopf CA. Multi-step planning of eye movements in visual search. Scientific reports. 2019;9(1):1–12.

36. Schwettmann S, Tenenbaum JB, Kanwisher N. Invariant representations of mass in the human brain. eLife. 2019;8:e46619.

37. Battaglia PW, Hamrick JB, Tenenbaum JB. Simulation as an engine of physical scene understanding. Proceedings of the National Academy of Sciences. 2013;110(45):18327–18332.

38. Zednik C, Jäkel F. Bayesian reverse-engineering considered as a research strategy for cognitive science. Synthese. 2016;193(12):3951–3985.

39. Tversky A, Kahneman D. Judgment under uncertainty: Heuristics and biases. science. 1974;185(4157):1124–1131.

40. Trommershäuser J, Maloney LT, Landy MS. Decision making, movement planning and statistical decision theory. Trends in cognitive sciences. 2008;12(8):291–297.

Supporting information

Puck Movement

From Newtonian physics we know the relationships between a change in momentum Δp by a force F exerted over a time Δt:

$$\Delta p = \mathrm{F}\,\Delta t \tag{6}$$

The impulse is transferred to a puck of mass m resulting in a change of speed Δv:

$$\Delta p = m\,\Delta v \tag{7}$$

As the puck is initially at rest, the release velocity v_0 when shooting the puck can therefore be expressed as:

$$v_0 = \frac{\mathrm{F}\,\Delta t}{m} \propto \Delta t \tag{8}$$

Therefore, in the simulations the change in momentum Δp increases linearly with press-time Δt and proportionally to force F and thus the initial velocity v_0 also scales linearly with the press-time. Once released, a frictional force F_{fr}, which can be expressed in terms of the gravitational force F_g and the friction coefficient μ:

$$F_{fr} = \mu F_g = \mu m g, \tag{9}$$

which slows the puck down with an acceleration a_{fr}, which accordingly to Newton's second law $F = ma$ is:

$$a_{fr} = \mu g \tag{10}$$

until at rest after some time T:

$$v_T = 0 = v_0 - a_{fr}T \tag{11}$$

During this time the puck has moved a distance s_T

$$s_T = \frac{1}{2}a_{fr}T^2 \tag{12}$$

Solving eq. 11 for T and substituting into eq. 12, substituting the acceleration a_{fr} from eq. 10 and using the expression for the initial velocity v_0 from eq. 8 allows finding the press-time required for propelling the puck over a distance Δx in eq. 1.

Position and velocity updates per frame:

We used the difference equations corresponding to the above equations of motion:

$$x_{t+\delta t} = x_t + v_t \delta t \tag{13}$$

$$v_{t+\delta t} = v_t - a_{fr}\delta t. \tag{14}$$

Distance error distributions
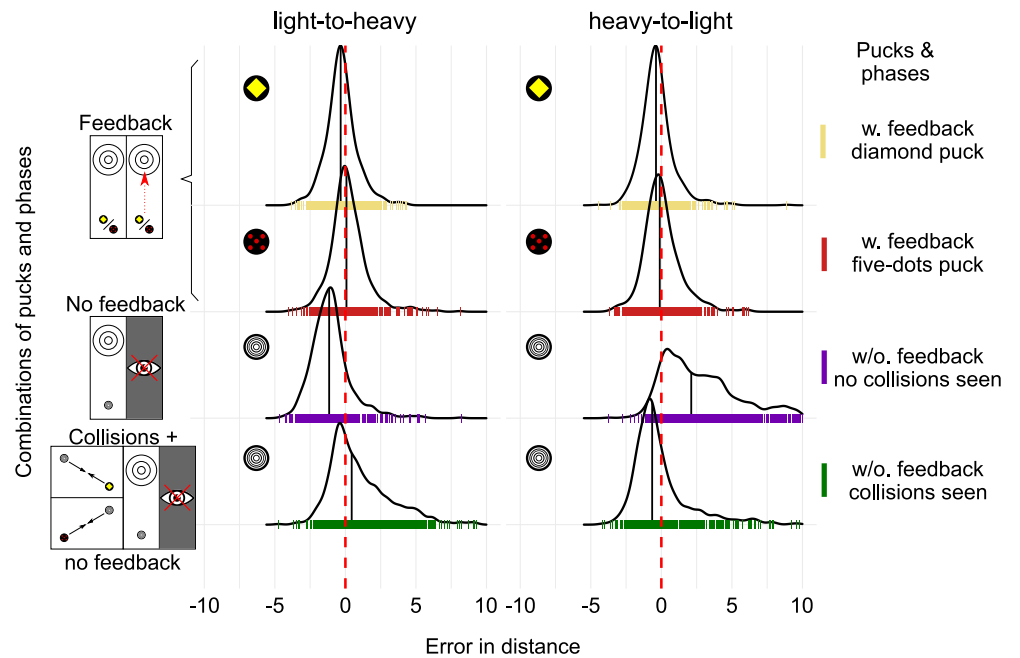
Fig 9. Distance error distributions. Final discrepancy between target and puck pooled for all participants. Pucks being shot too short are shown with negative values, pucks with a positive deviation were shot too far. Columns showing the the data for both conditions and rows divide into puck and phase combinations. The first two rows (in gold and red) showing the error distributions for both pucks with feedback in phase 2. The error distribution for the unknown puck in phase 3 before seeing the collisions is shown in the second last row (in purple) with greater deviation, with a clear bias and bigger spread. In the last row the error distributions are depicted for the unknown puck after having seen the collisions with the previous learned pucks, showing a reduced bias.

Press-time distributions
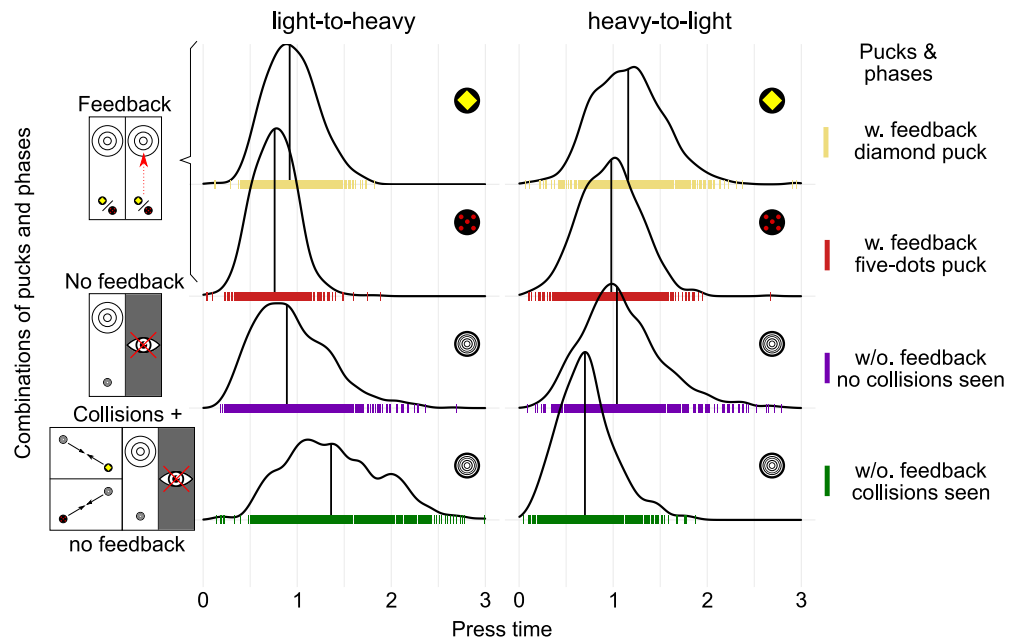
Fig 10. Press-time distributions. Pooled press-time distributions for all participants. Columns showing the the data for both conditions and rows divide into puck and phase combinations. First two rows showing the press-times for the pucks with feedback. Press-time distributions in phase 3 without feedback are shown in row three in blue. Without further information participants' behavior in phase 3 is strongly influenced by the previous phase and its press-time distribution: press-time distributions for the unknown puck in phase 3 reflect roughly the combined distributions of press-times of the previous pucks in phase 2 (Kolmogorov $D = 0.0538$; $p = 0.092$ for heavy-to-light, $D = 0.156$; $p = 9.8 \times 10^{-12}$ for light-to-heavy)

Kolmogorov tests - press-times in phase 2 & phase 3
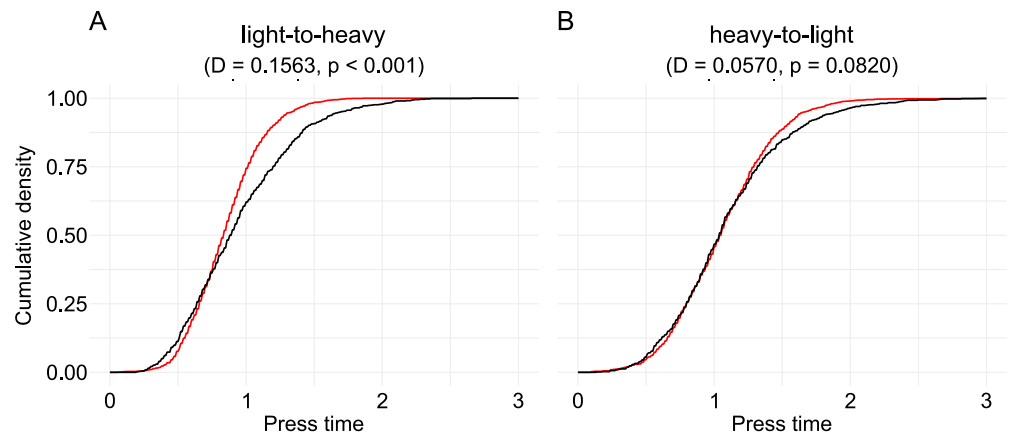
Fig 11. Empirical cumulative density function for press-time distributions of phase 2 and 3 for both conditions. (A) In the light-to-heavy condition both distributions of press times when seeing pucks and without feedback in phase 3 differ significantly. However, considering the asymmetry within the task response - press-times and potential masses are only constrained single-sided towards lower values with a minimum at zero - this difference in press-time distributions is surprisingly small. **(B)** In the heavy-to-light condition there was no significant difference between the distribution of press-times of both combined feedback pucks and the unknown puck before observing the collisions as revealed by the Kolmogorov-Smirnov test. This suggests that participants adhere to their previous adjusted strategies when facing decisions in great uncertainty.

Implementation of cost functions
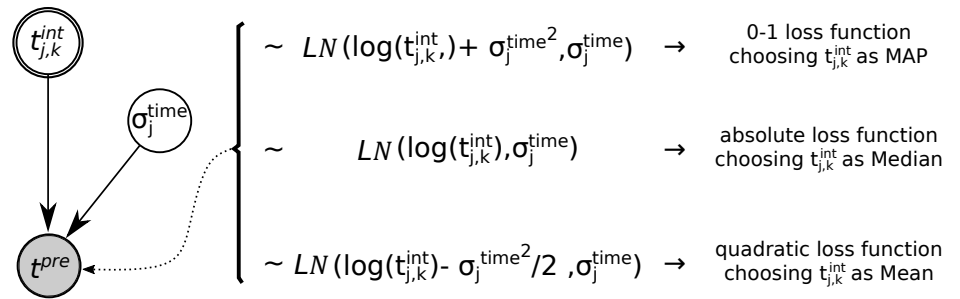
Fig 12. Implementation of three different cost functions - 1-0, absolute and quadratic loss.

Posterior predictive checks of cost functions in phase 2
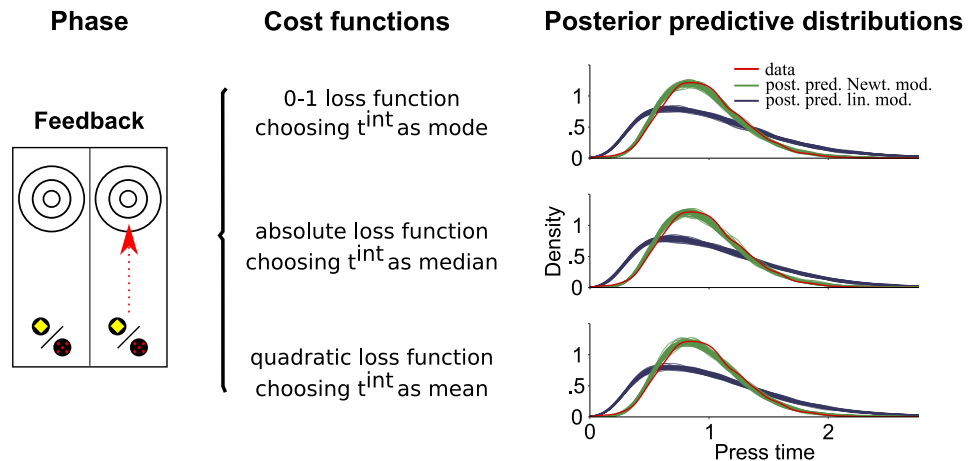
Fig 13. Posterior predictive distributions for both model classes and all cost functions with data from phase 2 with feedback. Posterior predictive distributions of press-times given data from feedback trials. Fifty distributions were drawn from each model after being fitted to the data. Dark green distributions arise from models of the Newtonian model class, dark blue ones from the linear model class. Separation into rows is made on basis of the implemented cost function. For each cost function the Newtonian model predicts values that match the actual data shown as red curve obviously better than the model from the linear model class.

Posterior predictive checks for press-times in both models
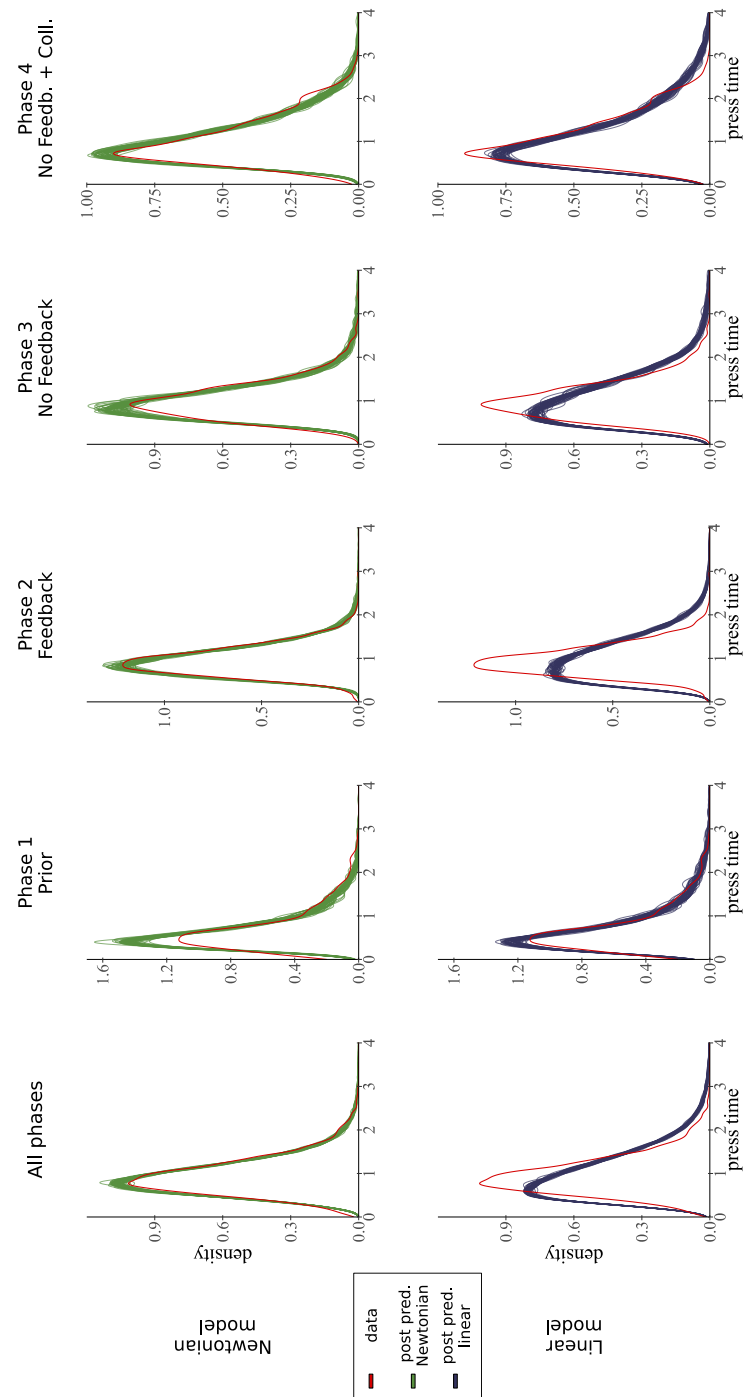
Fig 14. Posterior predictive checks for press-times in both models. Posterior press-time predictions for both, the linear and the Newtonian model with quadratic cost function, and separately for every phase. Actual data is shown as red line. Model predictions in dark green (50 iterations) of the fitted Newtonian model match the data closely and surpass the fitted linear model in dark blue for the complete data set and in almost every phase individually.

Latent masses by cost function: aggregated data from phase 2
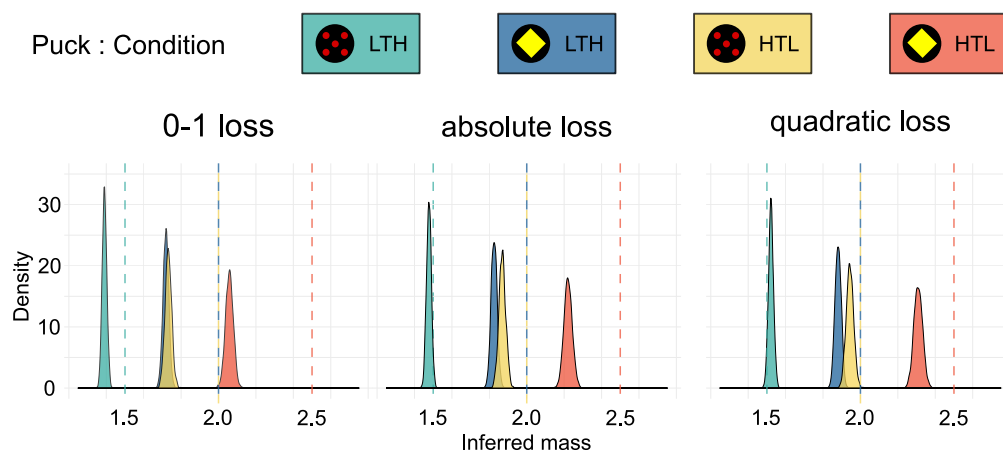
Fig 15. Inferred latent mass beliefs with aggregated data from phase 'feedback' for each cost function. Posterior distributions for mass belief aggregated over all participants for each cost function. Colored, vertical lines indicate actual mass of pucks. In comparison the quadratic loss function leads to posterior distributions that fit closest to the actual masses in the experiment.
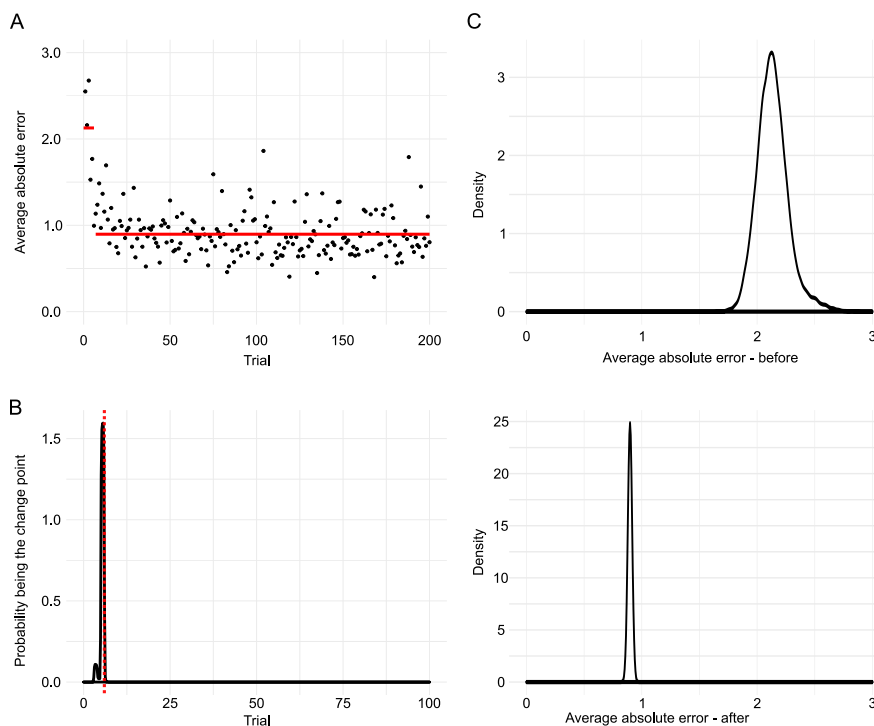
Change point detection

Fig 16. Average absolute error as function of trials and posterior of mean average error derived using the change point detection model. (A) Average absolute error over participants as function of trial number. **(B)** Posterior over change point τ. Red dotted line marks trial six. **(C)** Posterior of mean error before and after change point.

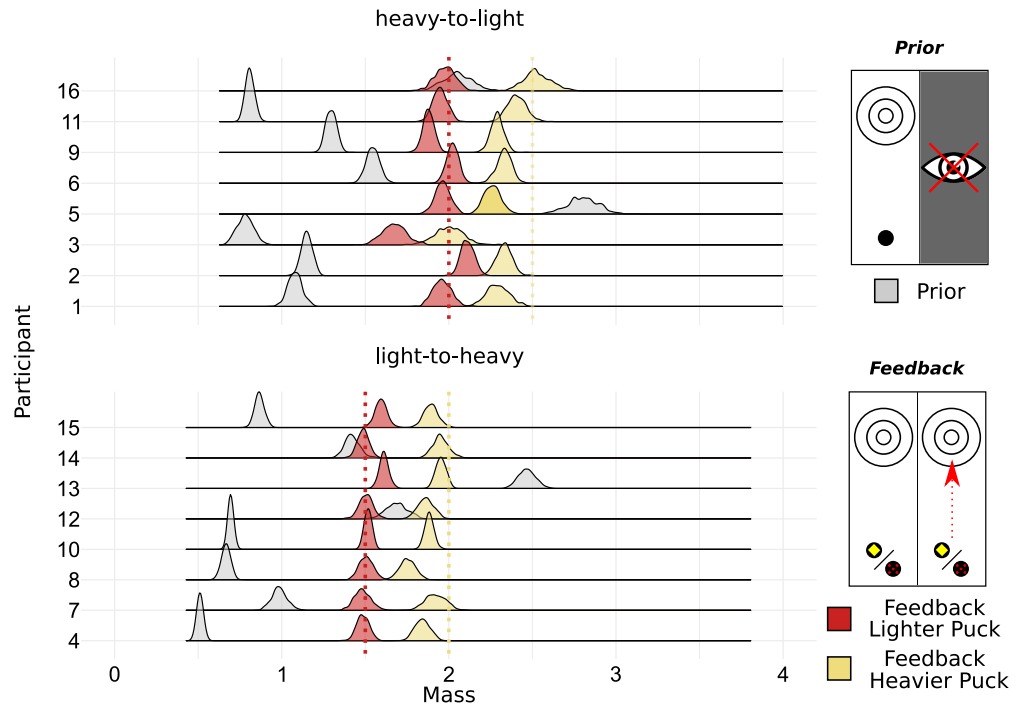## Latent masses: phase 'prior' and 'feedback'

Fig 17. Inferred latent mass in Newtonian model class with quadratic loss function for each participant and with data from *Prior* and *Feedback* phase. Posterior mass distributions for each participant in *Prior* and *Feedback* phase. Gray distributions show the inferred mass distribution for an unknown puck before participants have encountered the task dynamics. Resulting mass distributions for both pucks in feedback trials in red (light puck) and yellow (heavy puck). Dotted lines indicate actually implemented mass for each of the feedback pucks.

Latent masses: phase 'no feedback' and 'collision and no feedback'
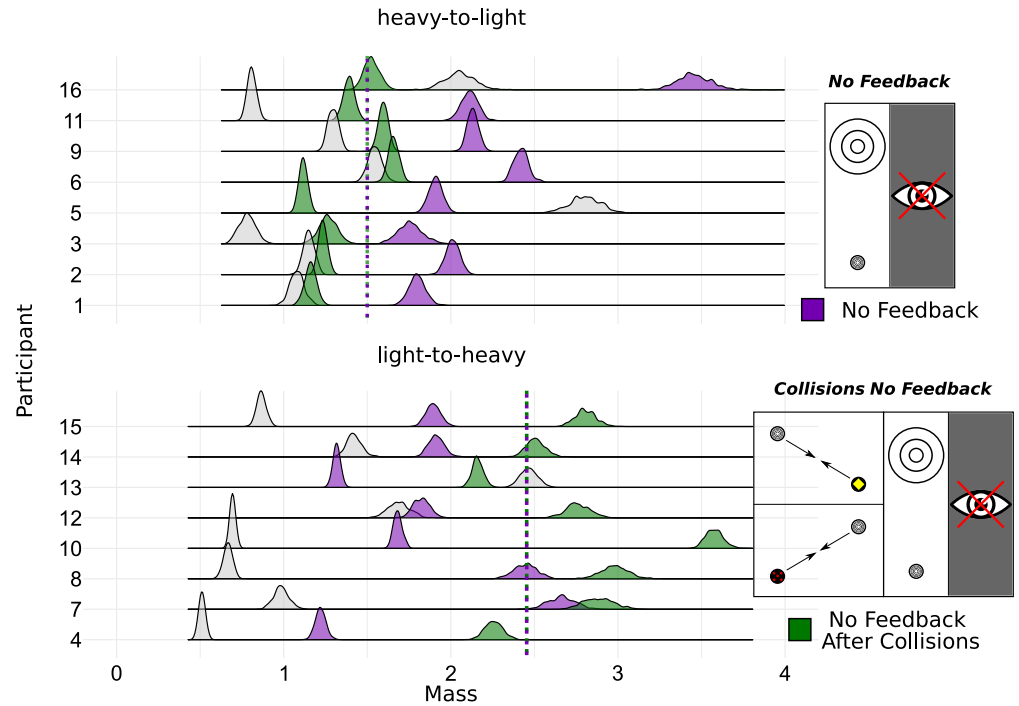

Fig 18. Inferred latent mass in Newtonian model class with quadratic loss function for each participant with data from *Prior* and both *No Feedback* phases. Posterior mass distributions for each participant in *Prior* and *Feedback* phase. Gray distributions show again the inferred mass distribution for an unknown puck before participants have encountered the task dynamics. Distributions in violet and green are the posterior mass distributions of the unknown puck without feedback before and after the participants saw collision with known pucks. Dotted line marks the actual mass of the unknown puck.
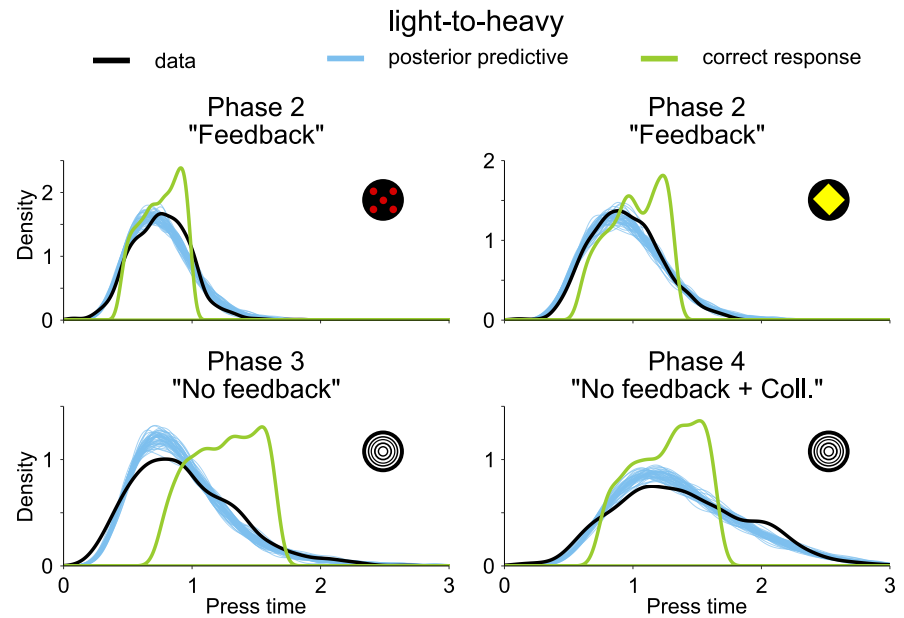
Fig 19. Posterior predicitve for press times, actual press times and ideal responses for phases two to four and condition light-to-heavy. Black distributions show the actual data, blue ones display samples from the posterior predictive distribution and green ones show the correct responses given perfect knowledge about the underlying physics and all parameters. Visualizing the enhanced suitability of this noisy Newtonian model framework compared to Newtonian models excluding prior preferences and uncertainties in describing human behavior.
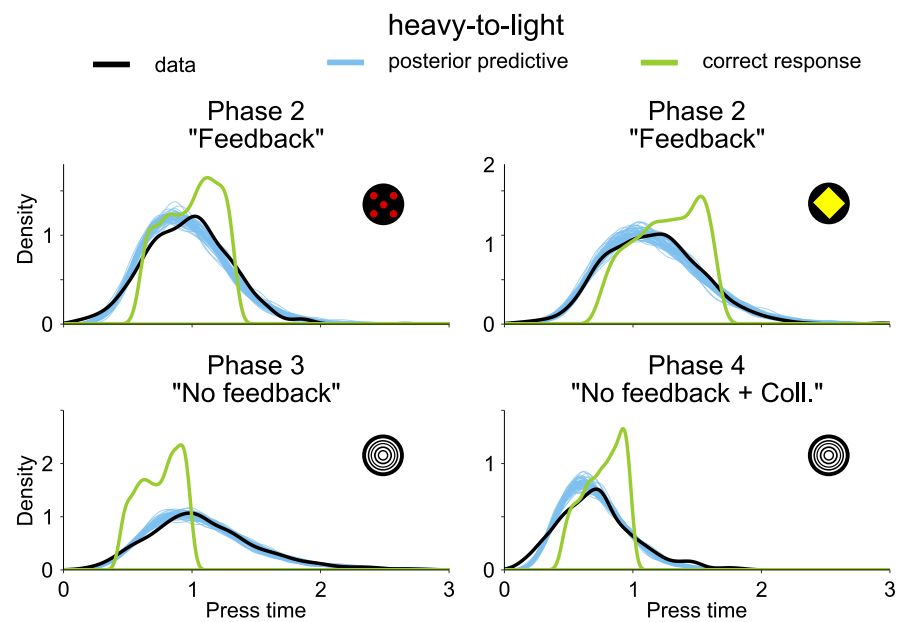
Fig 20. Posterior predicitve for press times, actual press times and ideal responses for phases two to four and condition heavy-to-light.